Pergamon

Int. J. Heat Mass Transfer. Vol. 40, No. 7, pp. 1693–1699, 1997

0017–9310/97 $17.00+0.00

PII: S0017–9310(96)00199–8

The mixed convection plume along a vertical adiabatic surface embedded in a non-Darcian porous medium

JIIN-YUH JANG and CHUAN-TZER SHIANG

Department of Mechanical Engineering, National Cheng-Kung University, Tainan, Taiwan 70101, Republic of China

(*Received* 10 *October* 1995)

Abstract—The mixed convection flow, from a line heat source embedded at the leading edge of an adiabatic vertical surface which is immersed in a non-Darcian porous medium, is numerically studied by employing an implicit finite difference Keller's box method. The non-Darcian effects of convective, inertia, and solid boundary are all considered. Both the buoyancy-assisting and buoyancy-opposing flow conditions have been investigated. The results are presented for the entire range of the mixed convection parameter $\Lambda_L = Gr_L/Re_L^2$, a ratio of the buoyancy-force to the inertia-force, from the purely force convection ($\Lambda_L = 0$) to the purely free convection ($\Lambda_L \to \infty$) regimes. It is shown that the non-Darcian effects decrease the peak velocities and increase the maximum temperatures. The criteria for the pure and mixed convection for a wall plume in porous media are established. Copyright © 1996 Elsevier Science Ltd.

INTRODUCTION

The study of a plume arising from a thermal energy source finds applications in several engineering fields such as: the disposal of nuclear wastes, hot-wire anemometry, volcanic eruption, electronic circuits, etc. The free and wall plumes, from a line or a point thermal source, in a viscous fluid have been studied extensively [1–3]. However, the analogous problems of free and wall plumes in a saturated porous medium have received rather less attention.

For free convections in a Darcian porous medium, Wooding [4] developed a boundary-layer theory for steady state natural convection from a line or point source in an infinite Darcian saturated porous medium. Lai [5] re-examined the same problem for a point source and obtained a closed form solution. Bejan [6] used a perturbation analysis to study the transient and steady natural convection from a point heat source at a low Rayleigh number in a Darcian porous medium of infinite extent. The steady point heat sources at low and high Rayleigh numbers in an unbounded Darcian porous medium were investigated by Hickox and Watts [7] and Hickox [8]. Afzal and Salam [9] studied the natural convection arising from a point source in a Darcian porous medium bounded by an adiabatic conical surface. Coupled heat and mass transfer by natural convection at low Rayleigh numbers in an infinite Darcian porous medium has been reported by Poulikakos [10] for a point source; by Larson and Poulikakos [11] for a line source; and Lai and Kulacki [12] for a sphere. For a large Rayleigh number, Lai [13] obtained the similarity solution for a line source.

For free convections in a non-Darcian porous medium, Ingham [14] obtained an exact solution for the free convection from a line source in an unbounded non-Darcian porous medium when only the inertia effect is considered. Local non-similarity solutions are reported by Lai [15] for natural convection from a line source to examine the inertia and thermal dispersion effects. Recently, the rigorous numerical solutions for the free plumes above line and point sources in non-Darcian porous media (combined convective, inertia and boundary viscous friction effects) were obtained by Leu and Jang [16, 17].

The thermal buoyancy force plays a significant role in forced convection, when the flow velocity is relatively low and the temperature difference between the surface and the free stream is relatively large. Under these conditions, mixed convection analysis is needed because the pure forced-convection or the pure free-convection analysis fails to predict the flow or heat transfer characteristics accurately. The Darcian mixed convection from a line thermal source embedded at the leading edge of an adiabatic vertical surface in a saturated porous medium was numerically analyzed by Kumari *et al.* [18]. Cheng and Zheng [19] used the local similarity method to study the mixed convection plume above a horizontal line source. The inertia and thermal dispersion effects are included. It should be noted that, to the authors' knowledge, the non-Darcian effects on the mixed convection wall plume from a line source has not yet been investigated. This has motivated the present investigation.

The object of the present work is to study the mixed convection flow due to a line thermal source imbedded at the leading edge of an adiabatic vertical plane

NOMENCLATURE

C	inertia coefficient
C_p	specific heat of fluid
f	dimensionless stream function
Gr_L	average modified Grashof number, $K^{1/2}g\beta T^* L^2/\nu^2$
g	gravitational acceleration
K	permeability
L	length of vertical plane
Pr	Prandtl number, ν/α_e
Q	strength of thermal line source per unit length
Re_k	dimensionless inertia parameter, CKu_∞/ν
Re_L	average Reynolds number, $u_\infty L/\nu$
Re_x	local Reynolds number, $u_\infty x/\nu$
T	temperature
T^*	characteristic temperature of thermal line source, $Q/\rho C_p \nu$
u, v	volume averaged velocity in x-, y-directions
x, y	distances along and perpendicular to the surface.

Greek symbols

α_e	effective thermal diffusivity of fluid-saturated porous medium
β	coefficient of thermal expansion
ε	porosity
η	pseudo similarity variable, $yRe_x^{1/2}/x$
Λ_L	mixed convection parameter, Gr_L/Re_L^2
μ	dynamic viscosity
ν	kinematic viscosity
θ	dimensionless temperature, $(T-T_\infty)Re_x^{1/2}/T^*$
Ψ	stream function
ρ	fluid density
ξ	non-similarity variable, $x^2 Re_x^{-1}/K$.

Subscript

∞	condition at the free stream.

immersed in a non-Darcian porous medium. The non-Darcian effects of convective, boundary and inertia are all considered. The governing partial differential equations are solved using a suitable variable transformation and employing an efficient finite-difference Keller's Box method [20] and the results are compared with those of the Darcy flow model [18]. Both the buoyancy-assisting and buoyancy-opposing flow conditions are considered. The criteria for the pure and mixed convection for a wall plume in porous media are established.

MATHEMATICAL ANALYSIS

We consider the mixed convection form a line heat source, generating heat a rate per unit length of Q, which is embedded at the leading edge of an adiabatic vertical plane surface placed in a saturated porous medium. The physical model and coordinate system are illustrated in Fig. 1. The forced flow is along the plane surface and the direction of the free stream velocity can be either assisting or opposing the buoyancy-induced convective velocity. In order to study transport through non-Darcian media, the original Darcy model is improved by including convective, boundary viscous and inertia effects. In addition, if we assume that: (1) the convective fluid and porous medium are in local thermal equilibrium; (2) variable porosity and thermal dispersion effects are neglected; (3) the Boussinesq and boundary-layer approximations are employed, then the governing equations become

$$\frac{\partial u}{\partial x}+\frac{\partial v}{\partial y}=0 \tag{1}$$

$$\frac{\rho}{\varepsilon^2}\left(u\frac{\partial u}{\partial x}+v\frac{\partial u}{\partial y}\right)=\pm\rho_\infty g\beta(T-T_\infty)-\frac{\mu}{K}(u-u_\infty)-\rho C(u^2-u_\infty^2)+\frac{\mu}{\varepsilon}\frac{\partial^2 u}{\partial y^2} \tag{2}$$

$$u\frac{\partial T}{\partial x}+v\frac{\partial T}{\partial y}=\alpha_e\frac{\partial^2 T}{\partial y^2} \tag{3}$$

where ε and K are the porosity and permeability of the porous medium, respectively; C is the transport property related to the inertia effect; α_e is the effective thermal diffusivity of the saturated porous medium. The other symbols are defined in the Nomenclature.

The '$\pm$' signs in equation (2) correspond to upward forced-flow (buoyancy-assisting) and downward forced-flow (buoyancy-opposing) conditions. The boundary conditions for equations (1)–(3) are

$$\begin{gathered} x=0 \quad y>0 \quad T=T_\infty \quad u=u_\infty \\ x>0 \quad y=0 \quad \frac{\partial T}{\partial y}=0 \quad u=0 \quad v=0 \\ y\to\infty \quad T=T_\infty \quad u=u_\infty. \end{gathered} \tag{4}$$

According to the principle of conservation of energy, at any position $x>0$, the convective energy should be equal to the energy released by the line heat source, Q. Thus

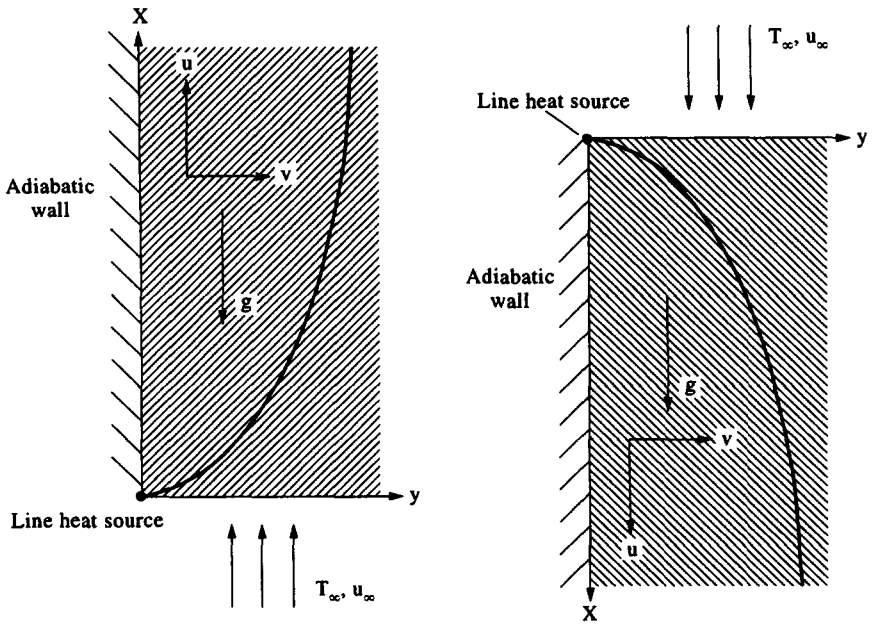

Fig. 1. The physical model and coordinate system.

$$Q = \rho C_p \int_0^\infty u(T - T_\infty)\,dy. \tag{5}$$

By using the scale analysis, we can introduce the following non-dimensional variables

$$\eta(x,y) = \frac{y}{x} Re_x^{1/2} \quad \xi(x) = \frac{x^2}{K} Re_x^{-1}$$

$$f(\xi,\eta) = \frac{\Psi(x,y)}{\nu Re_x^{1/2}} \quad \theta(\xi,\eta) = \frac{T - T_\infty}{T^*} Re_x^{1/2} \tag{6}$$

where $Re_x = u_\infty x/\nu$ is the local Reynolds number; $\Psi(x,y)$ is the stream function that satisfies equation (1) with $u = \partial\Psi/\partial y$ and $v = -\partial\Psi/\partial x$, and the characteristic temperature of the line source temperature T^* is defined as

$$T^* = Q/\rho C_p \nu. \tag{7}$$

Substituting equation (6) into equations (1)–(3), we obtain

$$\frac{1}{\varepsilon} f''' + \frac{1}{2\varepsilon^2} f f'' \pm \Lambda_L \xi^{1/2} \theta - \xi(f' - 1)$$

$$- Re_k \xi(f'^2 - 1) = \frac{\xi}{\varepsilon^2}\left(f' \frac{\partial f'}{\partial \xi} - f'' \frac{\partial f}{\partial \xi}\right) \tag{8}$$

$$\frac{1}{Pr}\theta'' + \frac{1}{2}(f'\theta + f\theta') = \xi\left(f' \frac{\partial \theta}{\partial \xi} - \theta' \frac{\partial f}{\partial \xi}\right) \tag{9}$$

where the primes denote partial differentiation with respect to η. $Pr = \nu/\alpha_e$ is the Prandtl number. $\Lambda_L = Gr_L/Re_L^2$ is the mixed convection parameter, which measures the relative importance of free to force convection. $\Lambda_L = 0$ corresponds to the case of purely force convection condition. $\Lambda_L \to \infty$ corresponds to the case of purely free convection condition. It is noted that Λ_L is not the function of x. $Gr_L = K^{1/2} g\beta T^* L^2/\nu^2$ is the average modified Grashof number. $Re_L = u_\infty L/\nu$ is the average Reynolds number. $Re_k = CKu_\infty/\nu$ is the dimensionless inertia parameter expressing the relative importance of the inertia effect. The '$\pm$' signs that appear on the left hand side of equation (8), denote the buoyancy-assisting plume and buoyancy-opposing plume. It is noted that Darcy's law [18] corresponds to the case of $\xi \to \infty$ with $Re_k = 0$.

The transformed boundary conditions for equations (8) and (9) are

$$\eta = 0 \quad f(\xi,0) = 0 \quad f'(\xi,0) = 0 \quad \theta'(\xi,0) = 0$$

$$\eta \to \infty \quad f'(\xi,\infty) = 1 \quad \theta(\xi,\infty) = 0 \tag{10}$$

and the transformation of equation (5) is

$$\int_0^\infty f'\theta\,d\eta = 1. \tag{11}$$

In terms of new variables, it can be shown that the dimensional velocity components and temperature are given by

$$u(x,y) = u_\infty f'(\xi,\eta)$$

$$v(x,y) = -\frac{\nu}{2x} Re_x^{1/2}\left(f - \eta f' + 2\xi \frac{\partial f}{\partial \xi}\right)$$

$$T(x,y) - T_\infty = T^* Re_x^{1/2} \theta(\xi,\eta)$$

$$= \frac{u_\infty^{3/2} \nu^{1/2}}{K^{1/2} g\beta x^{1/2}} \Lambda_L \theta(\xi,\eta). \tag{12}$$

NUMERICAL METHOD

In this study, the Keller's box finite-difference method was used. Equations (8) and (9) associated

with boundary conditions (10) and (11) were solved by an efficient and accurate implicit finite-difference method similar to that described in Cebeci and Bradshaw [20]. To begin with, the partial differential equations are first converted into a system of first-order equations; then these first-order equations are expressed in finite-difference forms in terms of center difference. Denoting the mesh points in the ξ–η plane by ξ_i and η_j where $i = 0, 1, \ldots, M$ and $j = 0, 1, \ldots, N$, this results in a set of nonlinear difference equations for the unknown at ξ_i in term of their values at ξ_{i-1}. The resulting nonlinear finite-difference equations are then solved by Newton' iterative method. The boundary-layer equations are thus solved step by step, by taking the converged solution at $\xi = \xi_{i-1}$. To initiate the process, equations (8) and (9) with $\xi = 0$ are first solved by using a sixth-order variable-step-size Runge–Kutta integration scheme. After obtaining a converged solution along $\xi = 0$, this solution is then employed in a Keller's box scheme with second-order accuracy to march step by step along the boundary layer.

We adopted the numerical algorithm [21] to deal with the integral constraint equation (11). We first drop the boundary conditions $f'(\xi, 0) = 0$ and $\theta'(\xi, 0) = 0$, then assume other presupposed boundary conditions $f''(\xi, 0) = s$ and $\theta(\xi, 0) = t$, where s and t are the undetermined nonzero constant. The refined values of s and t can be estimated by the Newton–Raphson method, associated with one set variation equations which were derived by taking the derivatives of the finite-difference equations of equations (8) and (9) and their boundary conditions (10) with respect to s and t. These variation equations can also be solved by using Keller's box scheme. The dropped boundary conditions, together with the integral condition, equation (11), are treated as constraints. The iterations for adjusting the presupposed boundary conditions are repeated until the following criterion, which is the sum of squares of the discrepancies for the constrained conditions, is satisfied:

$$H^2 + [f'(\xi, 0)]^2 + [\theta'(\xi, 0)]^2 \leqslant 10^{-8}. \quad (13)$$

In the calculation, the value of $\eta_\infty = 10$ was found to be sufficiently accurate for $|f'_\infty - 1| < 10^{-4}$ and $|\theta_\infty| < 10^{-4}$. Uniform step sizes of $\Delta\eta = 0.01$ in the η-direction were used. The step sizes of $\Delta\xi$ in the ξ-direction were also uniform, but $\Delta\xi$ depended on the value of Λ_L. As Λ_L is increased from 0–1000, $\Delta\xi$ is decreased in the range 0.05–0.0001.

RESULTS AND DISCUSSION

The three different solid–fluid combinations shown in Table 1 were used in this study. The values of permeability K and inertia coefficient C were calculated by employing the Ergun model [22]:

$$K = d^2\varepsilon^3/[150(1-\varepsilon)^2] \quad C = 1.75(1-\varepsilon)/\varepsilon^3 d.$$

Table 1. The three different solid–fluid combinations used in this study

Fluid	Air	Air	Air
Solid	Glass	Glass	Glass
d [mm]	3	6	15
ε	0.375	0.4	0.453
u_∞ [m/s^{-1}]	0.1	0.1	0.1
K [m^2]	8.1×10^{-9}	4.27×10^{-8}	4.66×10^{-7}
C [m^{-1}]	6913.6	2734.4	686.5
$Re_k = CKu_\infty/\nu$	0.3524	0.7342	2.0134

Figure 2 shows the different non-Darcy effects on the velocity and temperature profiles across the boundary layer for the buoyancy-assisting flow $\Lambda_L = 10$ at $\xi = 5$. The velocity profiles are referred to in the left and lower axes, while the temperature profiles are referred to in the right and upper axes. There are three cases included in this figure, they are the Darcy model [18], boundary effect (B) and the combined boundary and inertia effects (B + I). Therefore the boundary and inertia effects can be seen from the differences between the Darcy model and (B), and (B) and (B + I), respectively. It is seen that, as would be expected, both the boundary and inertia effects decrease the tangential velocities and increase the wall temperatures. The Darcy solutions overestimate the velocity and underestimate the maximum temperature.

Representative velocity and temperature profiles across the boundary layer for the buoyancy-assisting flow at different values of the mixing convection parameter Λ_L(= 1, 5 and 10) are presented in Fig. 3. The dashed lines represent the Darcy model [18]. From the definition of $\Lambda_L = Gr_L/Re_L^2 = K^{1/2}g\beta T^*/u_\infty^2$, the mixed convection parameter Λ_L depends on the source strength Q for the fixed value of u_∞. It is observed

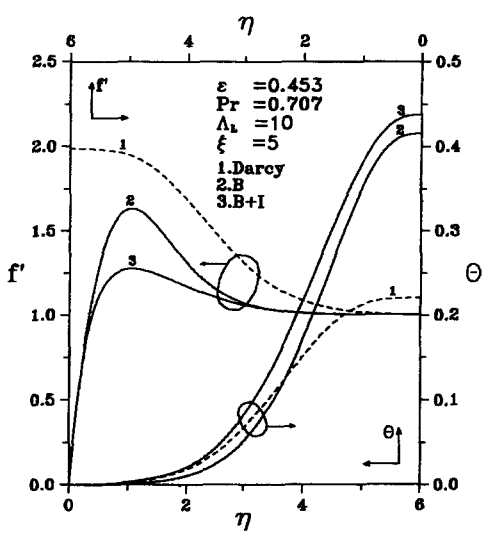

Fig. 2. Different non-Darcy effects on the velocity and temperature profiles for the buoyancy-assisting flow $\Lambda_L = 10$ at $\xi = 5$.

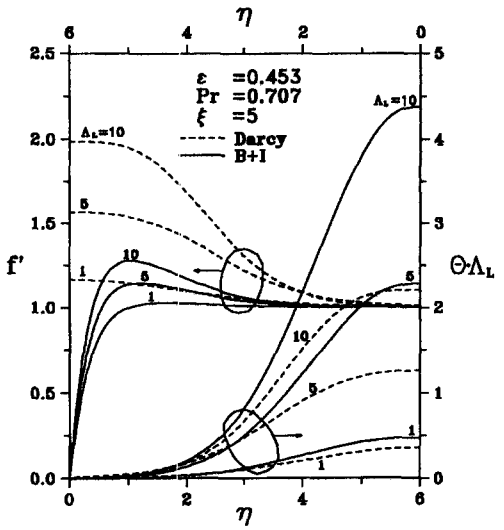

Fig. 3. The velocity and temperature profiles for the buoyancy-assisting flow at different values of mixing convection parameter Λ_L.

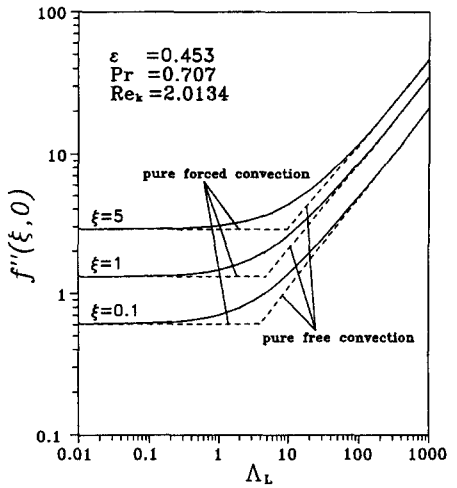

Fig. 5. The wall shear stress $f''(\xi, 0)$ for the buoyancy-assisting flow over the entire mixed convection regime, $0.01 \leqslant \Lambda_L \leqslant 1000$.

from Fig. 3 that for a fixed x and u_∞, the plume velocity, the velocity overshoot and the wall temperature increase as the mixed convection parameter Λ_L, or the source strength Q increases. In addition, the location of the maximum velocity moves closer to the adiabatic wall, thus causing an increase in wall shear stress. For $\Lambda_L = 10$, based on the (B+I) non-Darcy model, a 40% overshooting of the velocity beyond its free stream velocity is observed, while based on the Darcy model, the velocity is dramatically overshot by 100%. Moreover, it is seen that the discrepancy between the Darcy law [18] and the (B+I) model is large for large values of Λ_L.

Figure 4 shows the inertial effect ($Re_k = 0.3524$, 0.7342 and 2.0134) on the tangential velocity and temperature profiles at $\xi = 5$ for the buoyancy-assisting flow $\Lambda_L = 10$. Plotted with dashed lines in the figure, for comparison, are the results from the Darcy model [18]. It is seen that the inertia effect decreases the velocity and increases the temperature. This is because the form drag of the porous medium is increased, when the inertia effect is included.

The dimensionless wall shear stress $f''(\xi, 0)$ and the wall temperature $\theta(\xi, 0)$, for the buoyancy-assisting flow, are presented in Figs. 5 and 6, respectively, over the entire mixed convection regime $0.01 \leqslant \Lambda_L \leqslant 1000$. It is seen that the dimensionless wall shear stress $f''(\xi, 0)$ increases and the wall temperature $\theta(\xi, 0)$ decreases as the mixed convection parameter increases. The limiting cases of purely force convection ($\Lambda_L = 0$) and purely free convection [16] ($\Lambda_L \to \infty$) wall plumes are also shown as asymptotes in the same figures. They identify the region where both pure force and free convection results differ from the predicted mixed convection values. The criteria

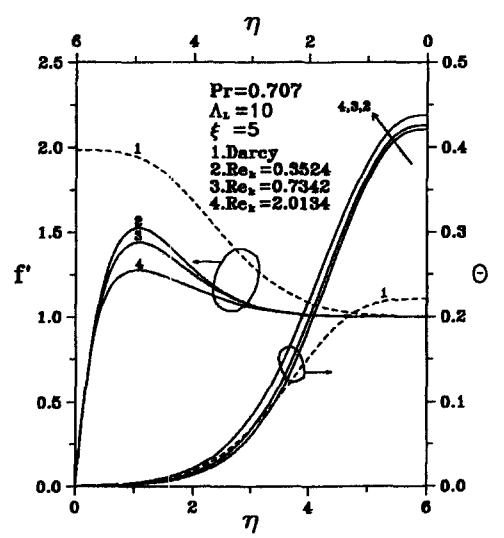

Fig. 4. The inertia effect on the tangential velocity and temperature profiles at $\xi = 5$ for the buoyancy-assisting flow $\Lambda_L = 10$.

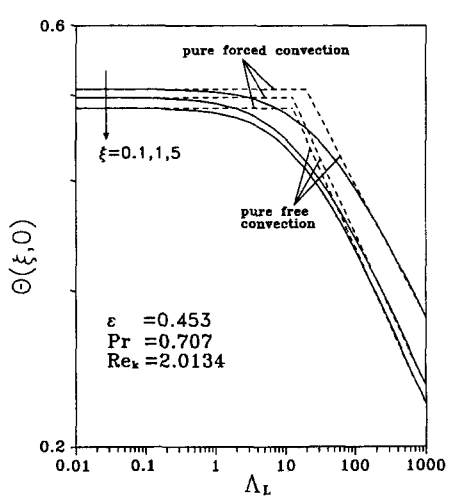

Fig. 6. The wall temperature $\theta(\xi, 0)$ for the buoyancy-assisting flow over the entire mixed convection regime, $0.01 \leqslant \Lambda_L \leqslant 1000$.

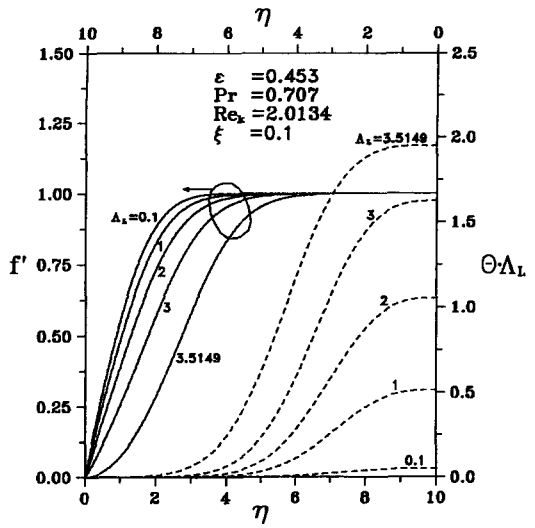

Fig. 7. The velocity and temperature distributions for the buoyancy-opposing flow condition at $\xi = 0.1$.

for pure or mixed convection about a wall plume can be established if the 5% deviation rule is applied. It follows that $0 < \Lambda_L < 0.1$ for purely force convection, $0.1 < \Lambda_L < 100$ for mixed convection and $\Lambda_L > 100$ for purely free convection.

The velocity and temperature distributions for the buoyancy-opposing flow condition are simultaneously presented at $\xi = 0.1$ and $\xi = 1$, respectively, in Figs. 7 and 8. As the source strength increases, the temperature and the plume width increase, but the velocity and wall shear stress decrease. Since the analysis is based on the boundary-layer approximations, only the buoyancy-opposing wall plume with slightly negative buoyancy can be studied. The present solutions terminate when the velocity gradient at the wall becomes close to zero, indicating an approach to flow separation. Flow separation occurs at $\Lambda_L = 3.5149$ for $\xi = 0.1$ and at $\Lambda_L = 5.1107$ for $\xi = 1$.

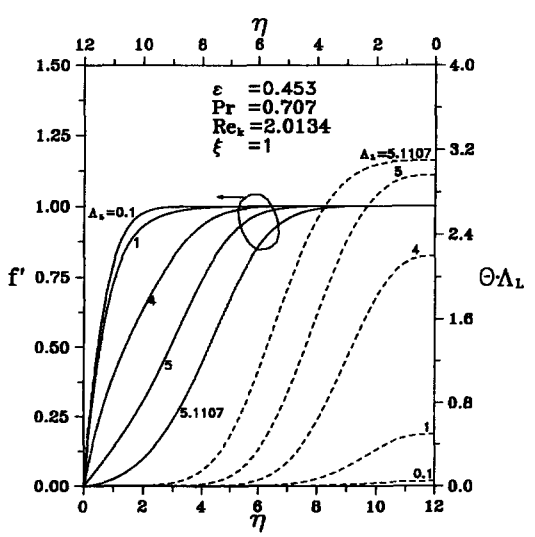

Fig. 8. The velocity and temperature distributions for the buoyancy-opposing flow condition at $\xi = 1$.

CONCLUSION

The non-Darcian effects are investigated for a wall plume from a line heat source embedded at the leading edge of an adiabatic vertical surface which is immersed in a saturated porous medium. The results are presented for the entire regime of mixed convection, from the purely force convection ($\Lambda_L = 0$) to the purely free convection ($\Lambda_L \to \infty$) regimes. It is shown that very large errors in transport prediction may arise from the Darcy model. The Darcy solutions overestimate the velocity and underestimate the maximum temperature. For the buoyancy-assisting flow, the wall temperature, velocity and wall shear stress increase, as the mixed convection parameter Λ_L or the source strength Q increases; while for the buoyancy-opposing flow, the wall temperature increases, but the velocity and wall shear stress decrease.

Acknowledgement—Financial support for this work was provided by the National Council of the Republic of China under contract NSC 84-2212-E006-014.

REFERENCES

1. Sparrow, E. M., Patankar, S. V. and Abdel-Wahed, R. M., Development of wall and free plumes above a heated vertical plate. *ASME Journal of Heat Transfer*, 1978, **100,** 184–190.
2. Rao, K. V., Armaly, B. F. and Chen, T. S., Analysis of laminar mixed convective plumes along vertical adiabatic surfaces. *ASME Journal of Heat Transfer*, 1984, **106,** 552–557.
3. Lin, H. T. and Chen. J. J., Mixed convection wall plumes. *International Journal of Heat and Mass Transfer*, 1987, **30,** 1721–1726.
4. Wooding, R. A., Convection in a saturated porous medium at large Rayleigh number or Peclet number. *Journal of Fluid Mechanics*, 1963, **15,** 527–544.
5. Lai, F. C., Natural convection from a concentrated heat source in a saturated porous medium. *International Communications in Heat & Mass Transfer*, 1990, **17,** 791–800.
6. Bejan, A., Natural convection in an infinite porous medium with a concentrated heat source. *Journal of Fluid Mechanics*, 1978, **89,** 97–107.
7. Hickox, C. E. and Watts, H. A., Steady thermal convection from a concentrated source in a porous medium. *ASME Journal of Heat Transfer*, 1980, **102,** 248–253.
8. Hickox, C. E., Thermal convection at low Rayleigh number from concentrated sources in porous medium. *ASME Journal of Heat Transfer*, 1981, **103,** 232–236.
9. Afzal, N. and Salam, M. Y., Natural convection from point source embedded in Darcian porous medium. *Fluid Dynamic Research*, 1990, **6,** 175–184.
10. Poulikakos, D., On buoyancy induced heat and mass transfer from a concentrated source in an infinite porous medium. *International Journal of Heat and Mass Transfer*, 1985, **28,** 621–629.
11. Larson, S. E. and Poulikakos, D., Double diffusion from a horizontal line source in an infinite porous medium. *International Journal of Heat and Mass Transfer*, 1986, **29,** 492–495.

12. Lai, F. C. and Kulacki, F. A., Coupled heat and mass transfer from a sphere buried in an infinite porous medium. *International Journal of Heat and Mass Transfer*, 1990, **33,** 209.
13. Lai, F. C., Coupled heat and mass transfer by natural convection from a horizontal line source in saturated porous medium. *International Communications in Heat and Mass Transfer*, 1990, **17,** 489–499.
14. Ingham, D. B., An exact solution for non-Darcy free convection from a horizontal line source of heat. *Thermal-and-Fluid Dynamics*, 1988, **22,** 125–127.
15. Lai, F. C., Non-Darcy natural convection from a line source of heat in saturated porous medium. *International Communications in Heat and Mass Transfer*, 1991, **18,** 445–457.
16. Leu, J. S. and Jang, J. Y., The wall and free plumes above a horizontal line source in non-Darcian porous media. *International Journal of Heat and Mass Transfer*, 1994, **37,** 1925–1933.
17. Leu, J. S. and Jang, J. Y., The natural convection from a point heat source embedded in a non-Darcian porous medium. *International Journal of Heat and Mass Transfer*, 1995, **38,** 1097–1104.
18. Kumari, M., Pop, I. and Nath, G., Darcian mixed convection plumes along vertical adiabatic surfaces in a saturated porous medium. *Thermal-and-Fluid Dynamics*, 1988, **22,** 173–178.
19. Cheng, P. and Zheng, T. M., Mixed convection in the thermal plume above a horizontal line source of heat in a porous medium of infinite extent. *Proceedings of the Eighth International Heat Transfer Conference*, Vol. 5, 1986, pp. 2671–2675.
20. Cebeci, T. and Bradshaw, P., Finite-difference solution of boundary-layer equations. In *Physical and Computational Aspect of Convective Heat Transfer*, Chap. 13. Springer, New York, 1984.
21. Yu, W. S., Lin, H. T. and Shih, H. C., Rigorous numerical solutions and correlations for two-dimensional laminar buoyant jets. *International Journal of Heat and Mass Transfer*, 1992, **35,** 1131–1141.
22. Ergun, S., Fluid flow through packed columns. *Chemical Engineering Progress*, 1952, 89–94.